Small molecule antagonists of melanopsin-mediated phototransduction

Kenneth A. Jones[1,*], Megumi Hatori[2,*], Ludovic S. Mure[2,*], Jayne R. Bramley[3], Roman Artymyshyn[1], Sang-Phyo Hong[1], Mohammad Marzabadi[1], Huailing Zhong[1], Jeffrey Sprouse[1,5], Quansheng Zhu[2], Andrew T.E. Hartwick[4], Patricia J. Sollars[3], Gary E. Pickard[3,6] & Satchidananda Panda[2]

Supplementary Information

Supplementary Results

Supplementary Figure 1. Melanopsin photosensitivity assay. (**a**) Schematic representation of various assays used in this study based on the melanopsin phototransduction mechanism. Melanopsin bound to *cis*-retinal forms a photopigment. Excitation by ~ 480 nm light source converts the retinal to all-*trans* retinal and activates Gq, which in turn activates phospholipase-C (PLC). PLC mediates conversion of PIP_2 to IP_3 and diacyl glycerol (DAG). IP_3 triggers calcium release from intracellular stores. (**i**) The transient increase in cytosolic calcium in melanopsin-expressing CHO cells was measured in a fluorescent plate reader by fluorescence from a calcium-sensitive Fluo-4 based dye which itself has peak excitation ~480 nm. (**ii**) Photoexcitation of melanopsin ectopically expressed in *Xenopus* oocytes leads to rise in DAG, which in turn acts upon a co-expressed TrpC3 channel and results in membrane depolarization, which can be measured by whole cell recording. (**iii**) In the native rat ipRGCs, melanopsin photoactivation generates action potentials and opening of voltage-dependent calcium channels leading to rise in intracellular calcium which can be measured by Fura-2 calcium indicator dye. (**b**) Light-induced increase in cytosolic Ca^{2+} in CHO cells expressing melanopsin (CHO^{Opn4}). Dark-adapted CHO^{Opn4} cells, but not the CHO cells, exhibited a light-induced transient increase in cytosolic Ca^{2+} measured by Fluo-4 based fluorescence. Exposing the CHO^{Opn4} cells to saturating levels of white light (1000 lx, 60 min) essentially abolished subsequent photoresponses, indicating inactivation of the melanopsin photopigment.

Supplementary Figure 2. Melanopsin photoresponse assay optimization. (**a**) Flow diagram of assay optimization and screen. For most of the experiments, the CHO^{Opn4} cells in serum-free medium were light-exposed on the day of the assay. All subsequent steps were carried out under darkness or dim red light. Relative temporal sequences of retinal or compound addition to light-exposed cells are shown. For acute addition of retinal, Ca^{2+} fluorescence from the cells were measured for 25 s and the retinal was acutely added inside the plate reader by a 384 pipette head. (**b**) Ca^{2+} fluorescence from light exposed CHO^{Opn4} cells in the first 25 s showed near complete inactivation of melanopsin. Photosensitivity was restored upon addition of retinal. (**c**) Ca^{2+} fluorescence from CHO^{Opn4} cells pre-incubated for 30 min with increasing concentrations of retinal. Note that light-evoked calcium responses occurred more quickly if 9-*cis* retinal was provided in the 30 min pre-incubation period, as compared to the acute addition protocol. (**d**) Difference spectra of purified bovine rhodopsin pre-incubated for 10 min with solvent, 3 μM or 6 μM opsinamide AA92593. After collection of dark spectrum, rhodopsin was light-exposed and another absorption spectrum was collected. Dark-light difference spectra are shown.

Supplementary Figure 3. Relationship between receptor binding and functional antagonism of opsinamides. (**a**) Linear correlation between binding affinity and functional antagonism for a series of sulfonamides. Binding affinity was measured by displacement of $[^3H]_2$- AA41612. pA_2 was calculated by measuring the right-ward shift in the 9-cis retinal concentration response curve caused by a fixed concentration of antagonist (1 or 10 μM) applied after bright light exposure using the FLIPR (see Fig. 2c for example). (**b**) Structure of opsinamides.

Supplementary Figure 4. General procedure for the preparation of substituted aryl-sulfonamides **1**-**6** and tritiation of 1-((2,5-dichloro-4-methoxyphenyl)sulfonyl)-1,2,3,6-tetrahydropyridine (compound **7**) to yield 1-((2,5-dichloro-4-methoxyphenyl)sulfonyl)piperidine-3,4-t_2 (Radio ligand $^3[H]_2$-AA41612) (compound **8**).

Supplementary Figure 5. Electroretinogram (ERG) of C57BL/6J mice treated with vehicle or opsinamides. Representative (out of 5 individual mice) ERG showing rod response, maximal combined rod and cone response and oscillatory potential from mice treated with vehicle or 30 mg kg^{-1} body weight of mouse treated with AA92593 20 min prior to the assay. The rod and cone responses from opsinamide treated retina were similar to those from vehicle treated retina.

Supplementary Figure 6. Opsinamide does not affect rod/cone photoresponse to successive light pulses of increasing intensity. (**a**) Electroretinograms of *Opn4*$^{-/-}$ mice in responses to 5 successive light pulses (0.006, 0.04, 0.25, 1.6 and 10 cd s/m^2, 250 ms each, separated by 2 min of darkness) were recorded. As expected, both the a and the b waves showed and increased amplitudes and reduction in onset latency with increasing light pulses intensity. The injection of compound 20 min before the first light pulse did not alter any of these 4 ERG parameters (average + SEM, n = 5, P > 0.05, Student's t test) at any of the 5 light intensities tested demonstrating an absence of adverse acute effect of the opsinamide AA92593 on rod or cone functions. (**b**) Opsinamide did not affect rod/cone photoresponse recovery after photobleaching. Mice electroretinograms (ERGs) in response to identical successive light pulses delivered 5 ansd 15 min after an intense 5 min saturating light exposition were recorded and normalized to a reference ERG recorded in response to a similar light flash delivered just before the bleaching exposure. 5 and 15 min after an extensive 5 min bleaching (e.g. 10 and 20 min after the reference ERG and the injection of the compound or the vehicle), the animals had only partially recovered the positive deflection of the ERG (15 - 20% and 25 - 30% after 5 and 15 min, respectively). The resulting waves maximum amplitudes and their delays were not different whether the animal was treated with the compound or vehicle alone (average + SEM, n = 5, P > 0.05, Student's t test) showing the absence of adverse effect of the opsinamide AA92593 on rod or cone functions in these conditions.

Supplementary Figure 7. Multielectrode array (MEA) recordings of the light-evoked responses during wash out. Examples of light-evoked (blue shading) responses over 30 min of 4 ipRGCs recorded from mice pretreated with vehicle (**a**) or mice pretreated with opsinamide (**b**). Note that discharge rates do not change over time in vehicle-treated mice whereas the light-evoked responses of ipRGCs pretreated with opsinamide gradually increase over time as opsinamide is washed out.

Supplementary Figure 8. Opsinamide affects the rate of pupil constriction in response to light and relaxation after cessation of light pulse. (**a** and **b**) A reproduction of Fig. 4A showed changes in pupil constriction in response to light has three major features which were influenced by the photopigment; constriction speed after the first 2 s, maximum constriction and relaxation rate. (**c** and **d**) In *rd* mice, opsinamides affected the rate of constrictions (**c**) and relaxation rate (mean constriction 60 s after lights off) (**d**) in response to light within 30 min of drug administration. As the drug was gradually cleared during the next hour, these response properties also returned to values as in vehicle-treated mice. (**e**) Average pupil diameter during the first 5 sec in response to bright light (10^{13} ph.cm^{-2}.s^{-1}). Dark adapted pupil diameter is normalized to 1. Data reproduced from Fig. 4c. Light pulse begins at t = 0 sec. Note, the initial constriction speed (first ~1 sec), previously shown to be independent of melanopsin, is similar in solvent and compound- treated WT mice.

Supplementary Figure 9. Central projections of ipRGCs in neonatal (P8) mouse. Serial coronal brain sections (100 μm thick) from a P8 *Opn4*$^{Cre/+}$*;Z/AP* mouse (*33*). These mice express Cre recombinase from the melanopsin locus, which activates Cre-inducible expression of human

alkaline phosphatase (AP) from β-actin promoter. AP present in the ipRGC axons can be visualized by a chromogenic dye. Coronal brain sections stained for AP (*33*) showed major ipRGC projections to various brain regions including the suprachiasmatic nucleus (SCN), hypothalamus, ventral and dorsal lateral geniculate nucleus (vLGN and dLGN), thalamus, intergeniculate leaflet (IGL), olivary pretectal nucleus (OPN), and superior colliculus (SC) are nearly complete by P8. OC, optic chiasma. OT, optic tract.

Supplementary Figure 10. Opsinamides inhibit negative phototaxis behavior of neonatal mice. Example of a WT pup injected with vehicle (**a**), WT pup injected with AA92593 (**b**), and *Opn4*$^{-/-}$ pup (**c**). Their activities are also shown in Supplementary movies 1-3.

Supplementary Table 1. Small molecule screening summary.

Supplementary Table 2. Binding and inhibition potency of several opsinamides against human melanopsin.

Supplementary Table 3. Potency and microsomal clearance rate of opsinamide AA92593.

Supplementary Table 4. Biological targets inhibited <30% by AA92593 at 10 μM concentration. The biological targets in appropriate assay conditions were tested for inhibition of specific radioligand binding by opsinamide AA92593 at 10 μM concentration. Less than 30% displacement of radioligand was observed for all 74 targets.

Supplementary Movie 1. Negative phototaxis of WT neonatal (P8) mouse treated with vehicle. The first 2 min of the movie showed the pup's activity inside a plexiglass tube under complete darkness. The next 2 min showed response to bright blue light illuminated from the left (shown as an arrow) of the plexiglass tube. Movie is sped 4X.

Supplementary Movie 2. Evaluation of negative phototaxis in WT neonatal (P8) mouse treated with AA92593. The first 2 min of the movie showed the pup's activity inside a plexiglass tube under complete darkness. The next 2 minutes showed response to bright blue light illuminated from the left (shown as an arrow) end of the plexiglass tube. Movie is sped 4X.

Supplementary Movie 3. Evaluation of negative phototaxis in neonatal (P8) *Opn4*$^{-/-}$ mouse. The first 2 min of the movie showed the pup's activity inside a plexiglass tube under complete darkness. The next 2 min showed response to bright blue light illuminated from the left (shown as an arrow) end of the plexiglass tube. Movie is sped 4X.

Supplementary Figure 1

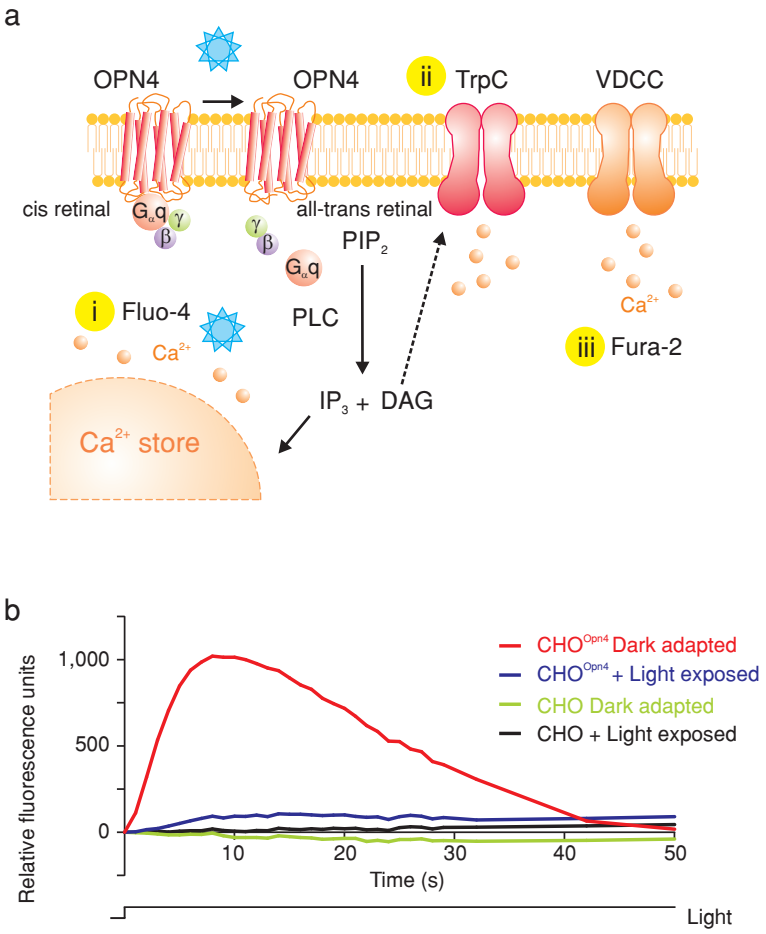

Supplementary Figure 2

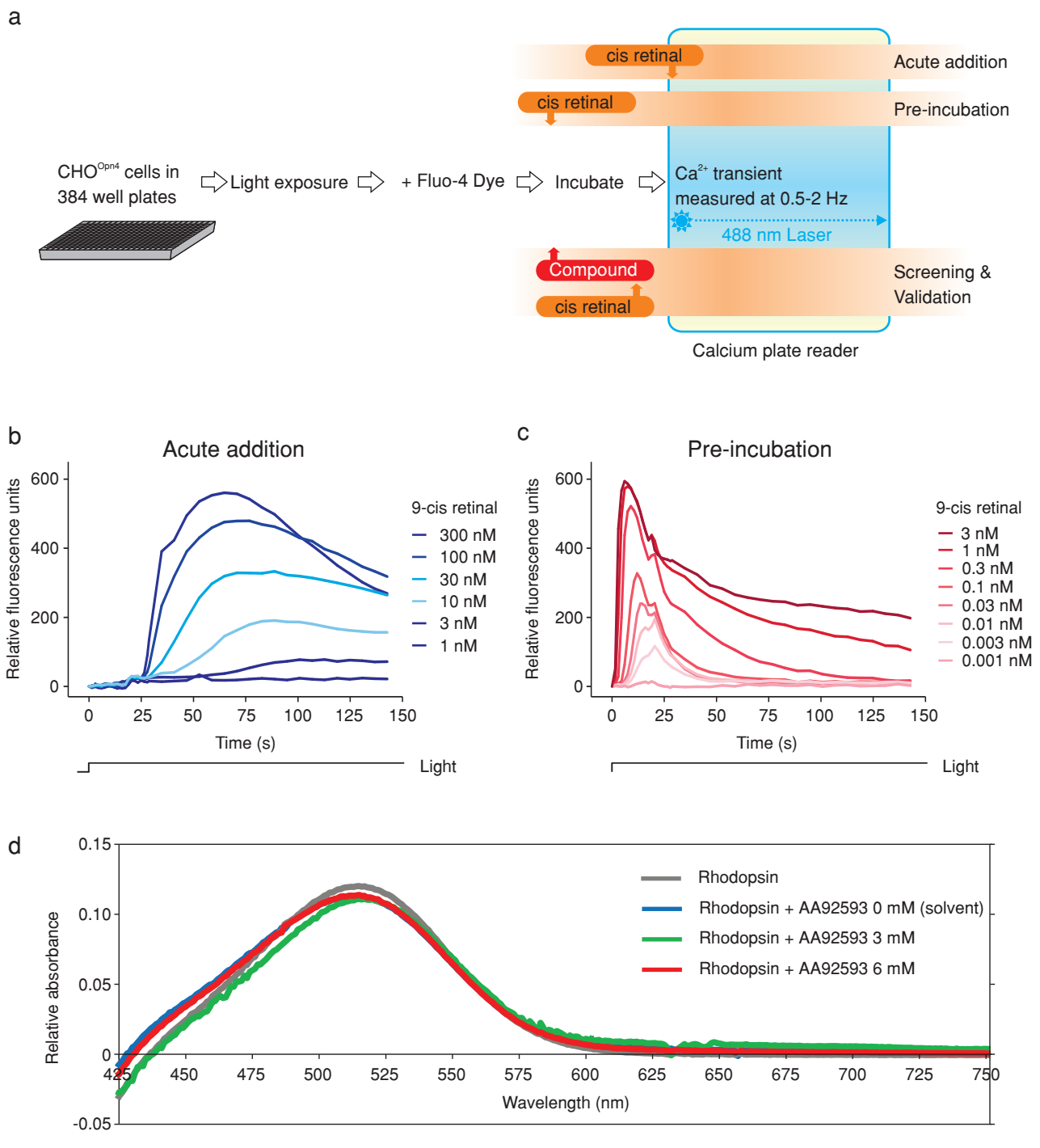

Supplementary Figure 3

a

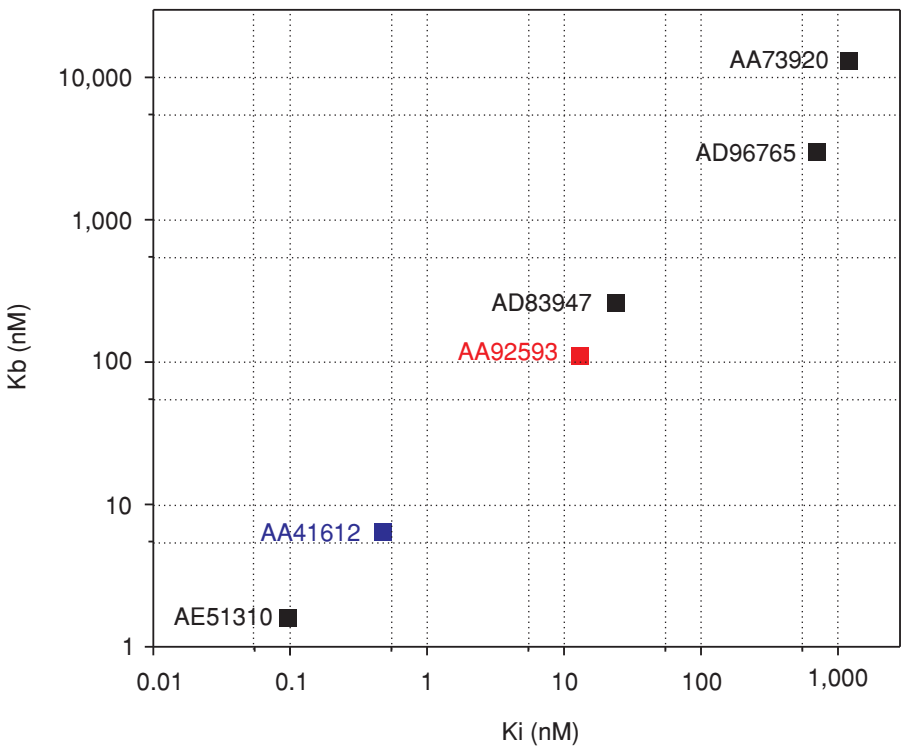

b

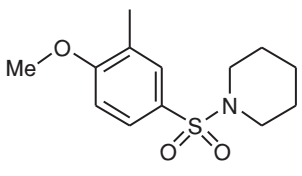

1
AA92593

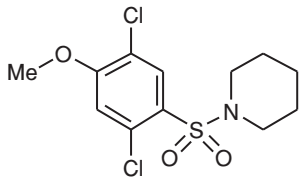

2
AA41612

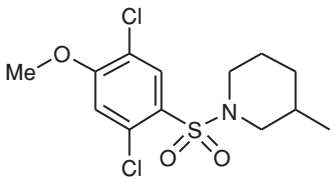

3
AE51310

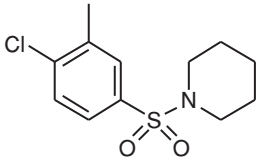

4
AD83947

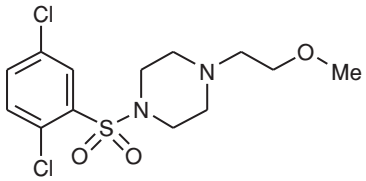

5
AD96765

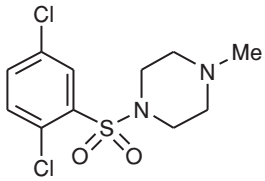

6
AA73920

Supplementary Figure 4

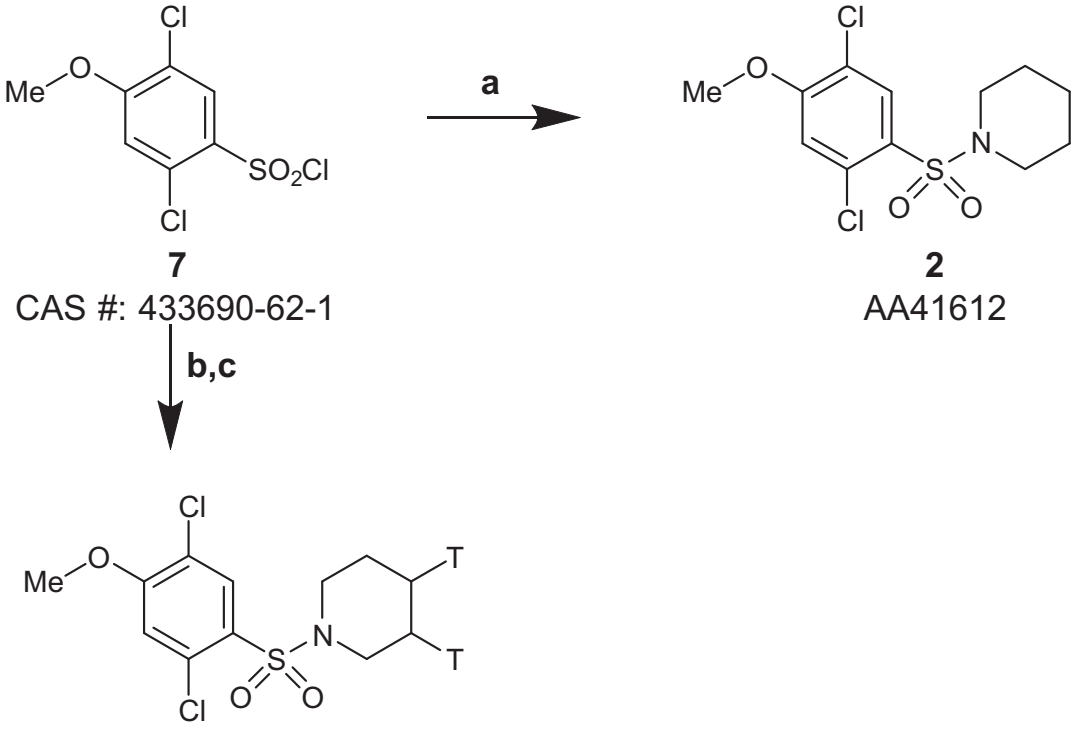

7
CAS #: 433690-62-1

2
AA41612

8
[^{3}H]-AA41612

a. piperidine, triethylamine, dichloromethane; *

b. 1,2,3,6-tetrahydropyridine, triethylamine, dichloromethane; *

c. T_2, Pd/C, ethyl acetate

* 2,5-dichloro-4-methoxybenzene-1-sulfonyl chloride (**7**) as well as the other arylsulfonyl chlorides / piperidines / piperazines used herein are commercially available

Supplementary Figure 5

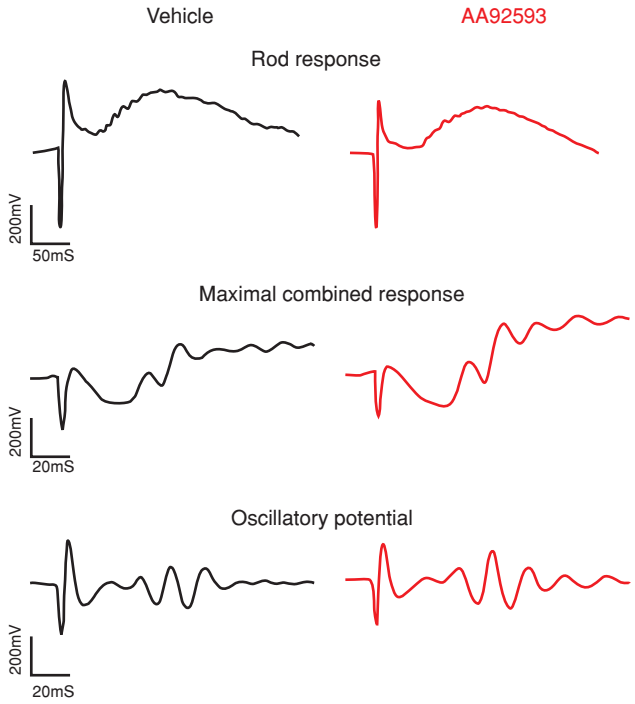

Supplementary Figure 6

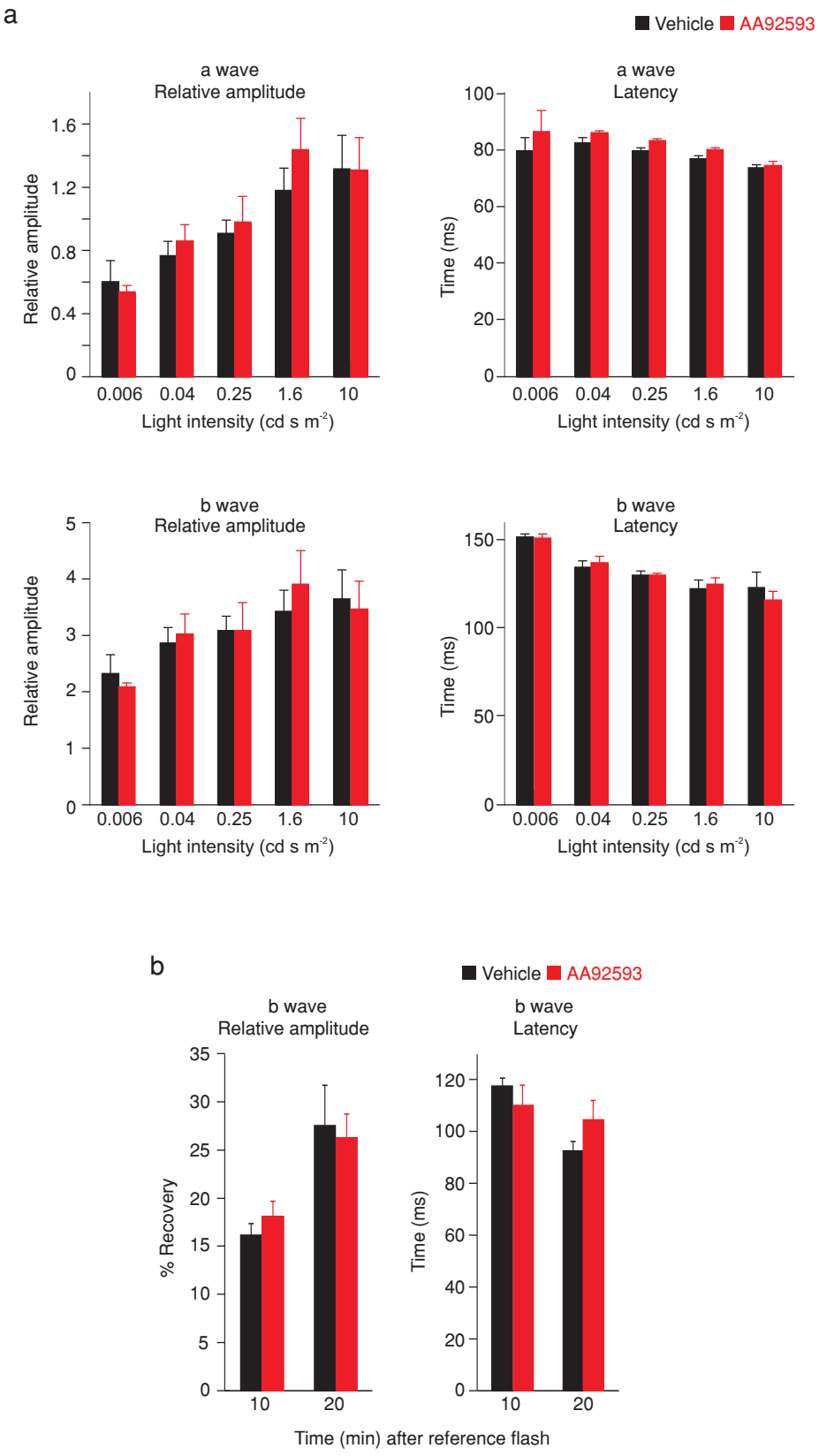

Supplementary Figure 7

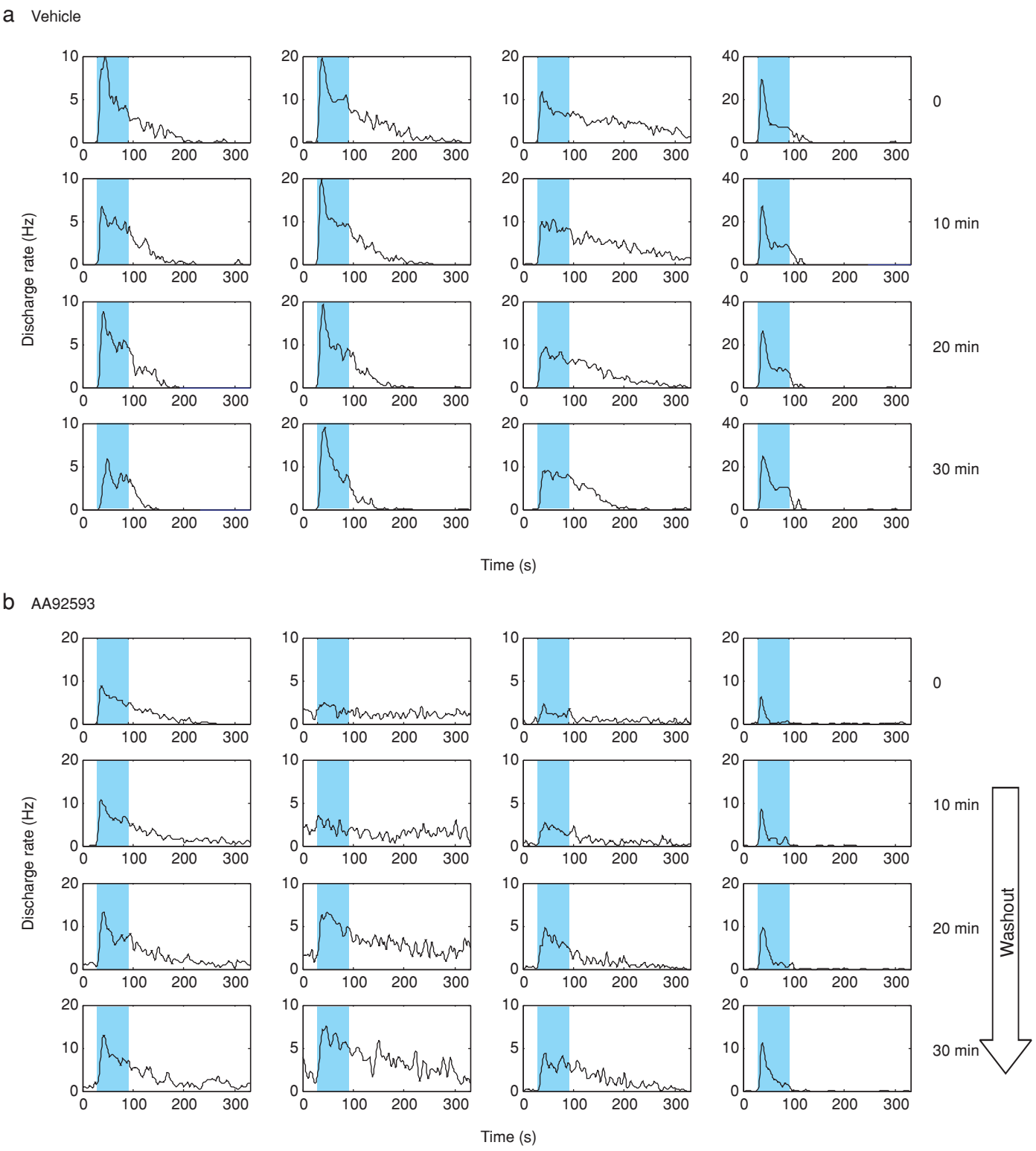

Supplementary Figure 8

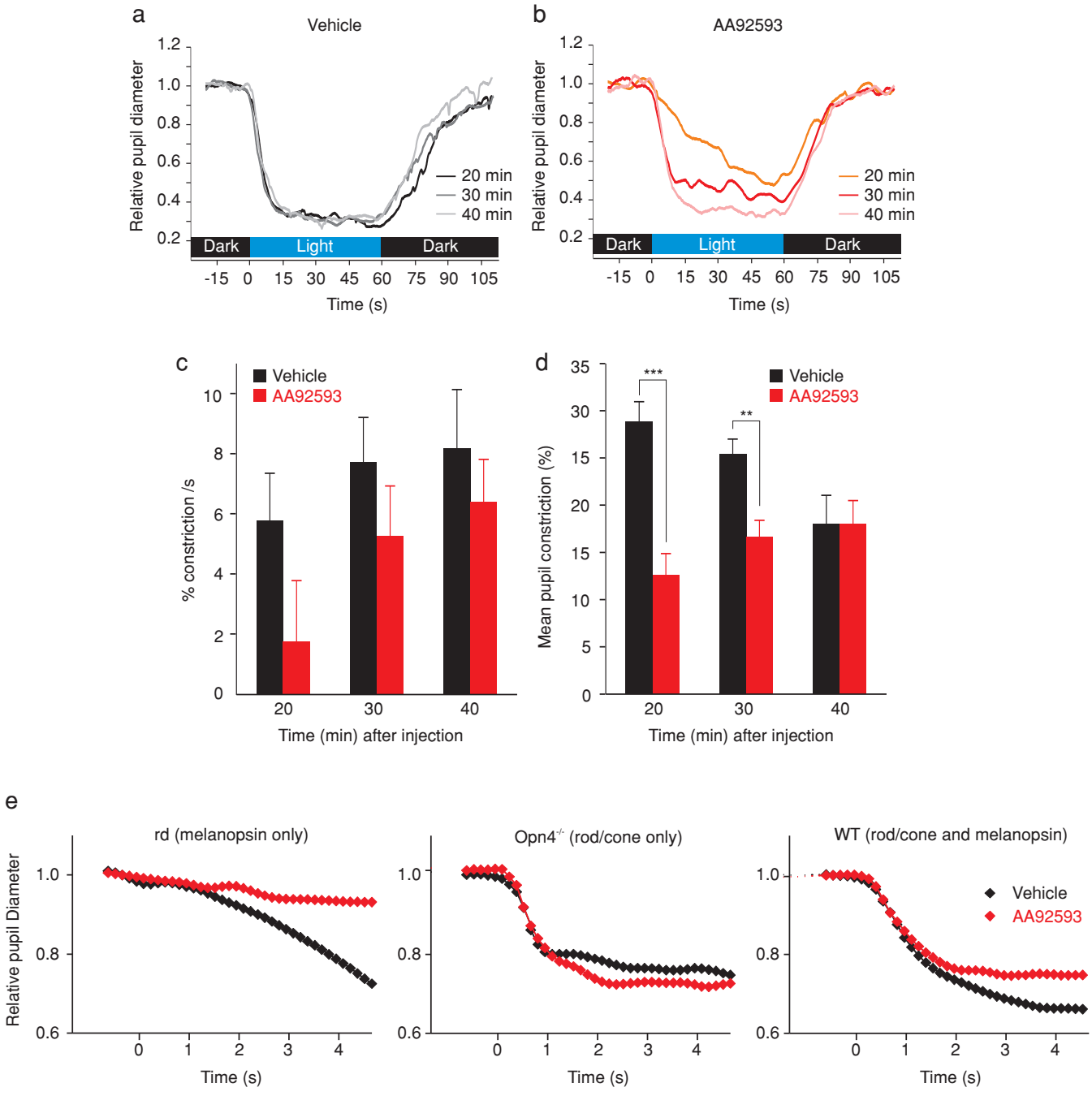

Supplementary Figure 9

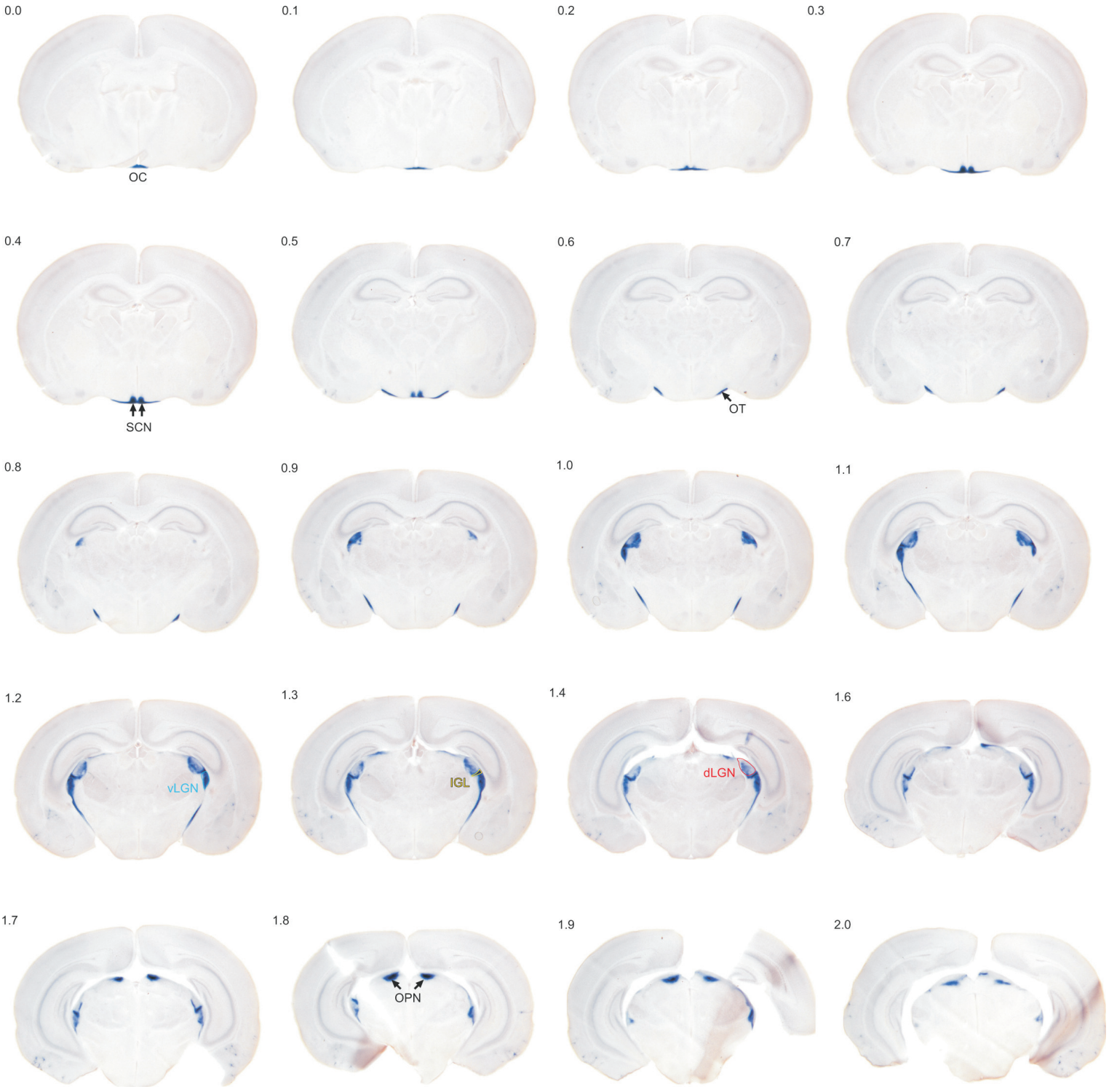

Supplementary Figure 10

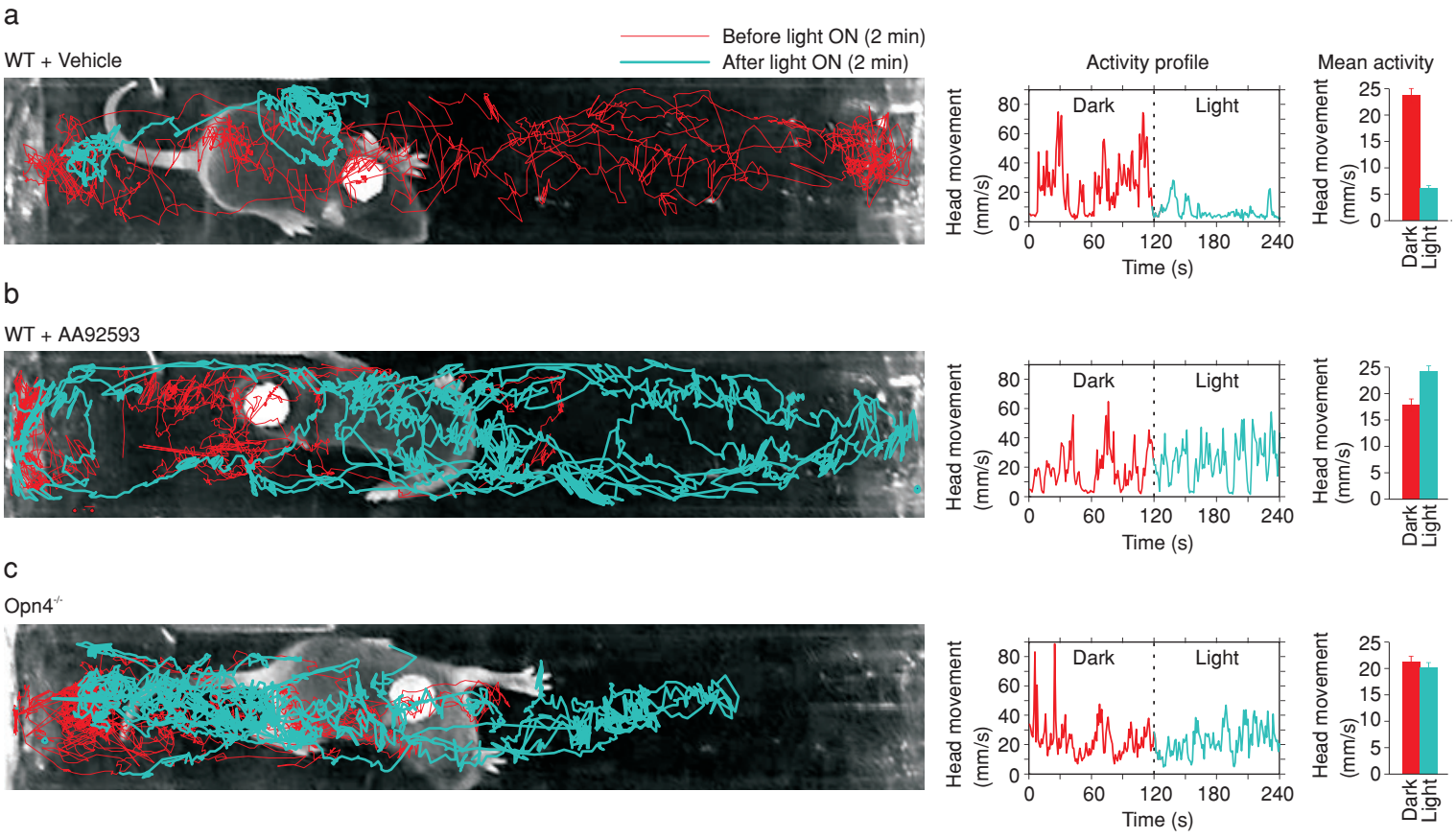

Supplementary Table 1. Small molecule screening summary

Category	Parameter	Description
Assay	Type of assay	Intracellular Ca^{2+} release using CHO^{OPN4}
	Target	Human and mouse OPN4
	Primary measurement	Light-stimulated increase in intracellular Ca^{2+}
	Key reagents	Fluo-4 indicator dye, CHO cells stably expressing OPN4, 9-cis retinal
	Assay protocol	See Methods section
	Additional comments	
Library	Library size	80,000
	Library composition	Drug-like small molecules
	Source	Lundbeck library (commercial and proprietary)
	Additional comments	
Screen	Format	384-well plate
	Concentration(s) tested	10 μM in 0.1% DMSO
	Plate controls	Positive controls ATP, 9-cis retinal; negative control buffer alone
	Reagent/ compound dispensing system	$FLIPR^{384}$
	Detection instrument and software	$FLIPR^{384}$
	Assay validation/QC	Z' > 0.7
	Correction factors	Not necessary
	Normalization	Baseline subtraction
Post-HTS analysis	Hit criteria	> 50% inhibition at 10 μM, sigmoidal concentration-effect curve, confirmation of compound ID and purity, activity in oocyte secondary assay
	Additional assay(s)	Radioligand binding using [^{3}H]-AA41612, oocyte voltage clamp
	Confirmation of hit purity and structure	LCMS

Supplementary Table 2. Binding and inhibition potency of several opsinamides against human melanopsin

Compound ID	Human OPN4 Ki (nM)	Human OPN4 Kb (nM)	Compound class
AA73920	1200	13000	Sulfonamide
AD96765	710	3000	Sulfonamide
AD84080	74	790	Sulfonamide
AD83947	24	260	Sulfonamide
AA92593	13	110	Sulfonamide
AA51307	1.9	89	Sulfonamide
AA41612	0.48	6.4	Sulfonamide
AE51310	0.096	1.6	Sulfonamide

Supplementary Table 3. Pharmacological and pharmacokinetic properties of AA92593

Opn4 Ki (nM)		Opn4 Kb (nM)			*In vitro* clearance (liver microsomes)		Plasma protein binding (% bound)	
Human	Mouse	Human	Mouse	Rat	Human (l/min)	Mouse (ml/min)	Human	Rat
13	47	110	160	250	49	39	95.8	94.9

Supplementary Table 4. Biological targets inhibited <30% by AA92593 at 10 uM

No.	Description	Human gene symbol
1	Adenosine A1 Receptor (Human)	ADORA1
2	Adenosine A2A Receptor (Human)	ADORA2A
3	Adenosine A3 Receptor (Human)	ADORA3
4	Adrenergic Alpha1A receptor	ADRA1A
5	Adrenergic Alpha2A receptor	ADRA2A
6	Adrenergic Beta1 receptor	ADRB1
7	Adrenergic Beta2 receptor	ADRB2
8	Angiotensin II Receptor, Type 1	AGTR1
9	Angiotensin II Receptor, Type 2	AGTR2
10	Arginine vasopressin receptor 1A	AVPR1A
11	Arginine vasopressin receptor 2	AVPR2
12	Bradykinin Receptor B1	BDKRB1
13	Bradykinin Receptor B2	BDKRB2
14	Cannabinoid Receptor 1	CNR1
15	Cannabinoid Receptor 2	CNR2
16	Cholecystokinin A Receptor	CCKAR
17	Cholecystokinin B Receptor	CCKBR
18	Corticotropin Releasing Hormone Receptor 1	CRHR1
19	Dopamine Receptor D1	DRD1
20	Dopamine Receptor D2	DRD2
21	Dopamine Receptor D3	DRD3
22	Dopamine Receptor D4	DRD4
23	Endothelin Receptor Type A	EDNRA
24	Endothelin Receptor Type B	EDNRB
25	Histamine Receptor H1	HRH1
26	Histamine Receptor H2	HRH2
27	Histamine Receptor H3	HRH3
28	Imidazoline I1 Receptor (Nischarin)	NISCH
29	Imidazoline I2 Receptor	
30	Leukotriene D4 Receptor (Cysteinyl Leukotriene Receptor 1)	CYSLTR1
31	Melanocortin 4 Receptor	MC4R
32	Muscarinic Receptor (non-selective) (cholinergic receptor, muscarinic 2)	CHRM2
33	Neurokinin (Substance P) Receptor	TACR1
34	Neuropeptide Y Receptor Y1	NPY1R
35	Opiate Receptor Like 1	OPRL1
36	Trachykinin (Neurokinin A) Receptor	TACR2
37	Trachykinin (Substance B) Receptor	TACR3

38	AMPA receptor	AMPAR
39	NMDA receptor	NMDAR
40	5-hydroxytryptamine Receptor	
41	Thyrotropin-Releasing Hormone Receptor	TRHR
42	Nuclear Receptor Subfamily 3, group C, member 1 (glucocorticoid receptor)	NR3C1
43	Estrogen Receptor 1	ESR1
44	Progesteron Receptor	PGR
45	Androgen Receptor	AR
46	Phosphodiesterase I	PDE1
47	Phosphodiesterase II	PDE2
48	Phosphodiesterase III	PDE3
49	Phosphodiesterase IV	PDE4
50	Phosphodiesterase V	PDE5
51	Adenylyl cyclase (basal)	
52	Guanylyl cyclase (basal)	
53	GABA A Receptor	GABAAR
54	Kainate Receptor	
55	Purinergic Receptor P2X, Ligand-gated Ion Channel	
56	Purinergic Receptor P2Y, Ligand-gated Ion Channel	
57	Voltage Dependent Calcium Channel (L type, 1,4-dihydropyridine sensitive or N binding site)	CACNA1C
58	ATP-sensitive potassium channel	KCNJ11
59	Small conductance calcium-activated potassium channels	
60	Sodium channel	
61	Chloride channel	
62	Norepinephrine transporter	SLC6A2
63	Dopamine transporter	SLC6A3
64	Sodium- and Chloride-dependent GABA transporter 1	SLC6A1
65	High-affinity Choline Transporter	SLC5A7
66	Serotonin Transporter	SLC6A4
67	Protein kinase C	PKC
68	Acetylcholinesterase (h)	AChE
69	Catechol-O-methyltransferase	COMT
70	4-aminobutyrate aminotransferase	ABAT
71	Monoamine oxidase A	MAOA
72	Monoamine oxidase B	MAOB
73	Phenylethanolamine N-methyltransferase	PNMT

74	Tyrosine hydroxylase	TH